7. Voronin, L. L. *Neuroscience* **56,** 275–304 (1993).
8. Kullman, D. M. & Nicoll, R. A. *Nature* **357,** 240–244 (1992).
9. Larkman, A., Hannay, T., Stratford, K. & Jack, J. *Nature* **360,** 70–73 (1992).
10. Stevens, C. F. & Wang, Y. *Nature* **371,** 704–707 (1994).
11. Mayer, M. L., Westbrook, G. L. & Guthrie, P. B. *Nature* **309,** 261–263 (1984).
12. Bekkers, J. M. & Stevens, C. F. *Nature* **341,** 230–233 (1989).
13. Muller, D., Joly, M. & Lynch, G. *Science* **242,** 1694–1697 (1988).
14. Kauer, J. A., Malenka, R. C. & Nicoll, R. A. *Neuron* **1,** 911–917 (1988).
15. Malgaroli, A. & Tsien, R. W. *Nature* **357,** 134–139 (1992).
16. Davies, S., Lester, R., Reyman, K. & Collingridge, G. *Nature* **330,** 500–503 (1989).
17. Aztely, F., Wigstrom, H. & Gustafsson, B. *Eur. J. Neurosci.* **4,** 681–690 (1992).
18. Maren, S., Tocco, G., Standley, S., Baudry, M. & Thompson, R. *Proc. natn. Acad. Sci. U.S.A.* **90,** 9654–9658 (1993).
19. McNaughton, B. L. *J. Physiol., Lond.* **324,** 249–262 (1982).
20. Wheeler, D. B., Randall, A. & Tsien, R. W. *Science* **264,** 107–111 (1994).
21. Wu, L. G. & Saggau, P. *J. Neurosci.* **14,** 645–654 (1994).
22. Manabe, T. & Nicoll, R. *Science* **265,** 1888 (1994).
23. Bashir, Z. I., Alford, S., Davies, S. N., Randall, A. D. & Collingridge, G. L. *Nature* **349,** 156–158 (1991).
24. Xie, X., Berger, T. W. & Barrionuevo, G. *J. Neurophysiol.* **67,** 1009–1013 (1992).
25. Tsien, R. W. & Malinow, R. *Cold Spring Harb. Symp. quant. Biol.* **55,** 147–159 (1990).
26. Dolphin, A., Errington, M. & Bliss, T. V. P. *Nature* **297,** 496 (1982).
27. Hessler, N. A., Shirke, A. M. & Malinow, R. *Nature* **366,** 569–572 (1993).
28. Hestrin, S., Sah, P. & Nicoll, R. *Neuron* **5,** 247–253 (1990).
29. Boulter, J. *et al. Science* **249,** 1033–1037 (1990).
30. Lynch, G. & Baudry, M. *Science* **224,** 1057–1063 (1984).

ACKNOWLEDGEMENTS. This work was supported by grant R29MH49159 to R.M.

Properties of synaptic transmission at single hippocampal synaptic boutons

Guosong Liu & Richard W. Tsien*

Department of Molecular and Cellular Physiology, Stanford University Medical Center, Stanford, California 94305, USA

SYNAPTIC transmission between individual presynaptic terminals and postsynaptic dendrites is a fundamental element of communication among central nervous system neurons. Yet little is known about evoked neurotransmission at the level of single presynaptic boutons[1–5]. Here we describe key functional characteristics of individual presynaptic boutons of hippocampal neurons in culture. Excitatory postsynaptic currents (e.p.s.cs) were evoked by localized application of elevated K^+/Ca^{2+} solution to single functional boutons, visually identified by staining with the vital dye FM1-43 (refs 6, 7). Frequent repetitive stimulation produced a decline in the incidence of e.p.s.cs as the pool of releasable vesicles was exhausted; typically, recovery proceeded with a time constant of about 40 s (23 °C), and involved a vesicular pool capable of generating about 90 e.p.s.cs without recycling. At individual synapses, synaptic currents were broadly distributed in amplitude[1], but this distribution was remarkably similar at multiple synapses on a given postsynaptic neuron. The average size of synaptic currents and of responses to focal glutamate application varied fourfold across different cells, decreasing markedly with increasingly dense synaptic innervation. This raises the possibility of a very effective mechanism for coordinating synaptic strength at multiple sites throughout the dendritic tree.

In studying hippocampal synapses in culture[1,8], one successful case was found in which local application of hypertonic sucrose activated a single presynaptic bouton[1]. We found that such activity could be isolated regularly by visualizing functional boutons with the styryl dye FM1-43 (refs 6, 7), then focally stimulating them with a puffer pipette while evoked e.p.s.cs were recorded under whole-cell voltage clamp (Fig. 1*a*). The puffer pipette contained 70–90 mM K^+ and 2 mM Ca^{2+} to depolarize the presynaptic membrane and allow Ca^{2+} entry, whereas spontaneous events elsewhere were minimized by superfusion with 0.2 mM Ca^{2+} external solution. The number of evoked e.p.s.cs was maximal when the puffer pipette tip was centred on the fluorescent area (Fig. 1*b*, trace 2), and markedly diminished if it was moved to either side (traces 1, 3). A 2 μm offset from the optimum position was sufficient to reduce strongly the evoked response when the interbouton spacing allowed a suitable test ($n=6$). A similarly sharp fall-off was seen in postsynaptic responsivity, assessed by direct application of glutamate from an iontophoretic pipette[9] (Fig. 1*c*). Small lateral movements of the pipette away from the dye-labelled bouton greatly diminished the glutamate response. Thus, with guidance from FM1-43 staining, either presynaptic terminals or postsynaptic receptor sites can be focally stimulated. The local nature of the presynaptic stimulation was corroborated by comparing fluorescent signals at adjacent single boutons (Fig. 1*d*). Puffer solution directed at bouton 1 decreased its fluorescence and caused the appearance of synaptic events[10], whereas fluorescence of bouton 2, ~3 μm away, remained unchanged. Out of ~80 whole-cell recordings with local K^+/Ca^{2+} stimulation, 14 satisfied this criterion for isolation of single bouton activity. When boutons were spaced by <3 μm, the local stimulation procedure typically destained groups of 2 or 3 boutons.

Figure 1*e–g* shows characteristics of the synaptic transmission from single boutons. The incidence of e.p.s.cs rose with a marked delay after initiation of pressure application and fell off sharply after its cessation (Fig. 1*e*), as expected for gradual settling of $[K^+]$ and $[Ca^{2+}]$ and for steep dependences of secretion on both concentrations[11–13]. The individual e.p.s.cs are quite similar in waveform although highly variable in amplitude (Fig. 1*f*). The evoked events rose rapidly (20–80% rise time, 0.46 ± 0.01 ms) and decayed quickly ($\tau=2.4\pm0.07$ ms, $n=186$). The incidence of evoked e.p.s.cs was highly Ca^{2+}-sensitive, as shown by alternately applying high K^+ solutions containing 2 or 0.3 mM Ca^{2+} to the same bouton (Fig. 1*g*). These characteristics are consistent with those expected for fast glutamatergic synaptic transmission[14,15].

Knowledge of the functional capabilities of nerve terminals of central nervous system (CNS) neurons is limited, although morphological characterization is extensive[3]. Local K^+/Ca^{2+} stimuli were effective in challenging this functional capacity[16]. When we presented trains of stimuli at appropriate frequencies (such as 0.2–0.5 Hz, Fig. 2*a*), the number of evoked events per trial declined sharply, suggesting a substantial depletion of the vesicular store. The decline is exponential at both frequencies but, at the higher frequency, the response reaches a lower steady state and requires more trials to settle. Both differences are quantitatively consistent with diminished recovery of vesicle availability during abbreviated interstimulus periods (Fig. 2 legend). The kinetics of recovery were studied by varying the rest interval t_r between trains of repetitive stimuli (Fig. 2*b*). The incidence of events during the second (test) train gradually recovered in degree as t_r was prolonged, but always decayed with the same time constant, consistent with a linear relationship between pool content and release rate. The recovery time course followed a single exponential, $\tau_r\sim40$ s. These characteristics are consistent with a model (inset, Fig. 2*b*) which generates the smooth curves fitted to the data. For simplicity, the model divides functional synaptic vesicles into two pools, unavailable and available (including both immediately releasable and reserve vesicles[16,17]). N designates the number of events that could be generated by the available pool at any given moment in the absence of vesicular reuse. N is governed by forward (ϕ) and reverse (ρ) transition probabilities between the pools and its initial value after a long rest is N_a. In 10 putative single bouton recordings, the average value of N_a was 93 ± 11 events (range 42–164). N_a could be interpreted as an estimate of the total number of functionally available vesicles per bouton, possibly only a lower limit because Ca^{2+} channel inactivation may have contributed somewhat to the declining response and some unitary e.p.s.cs might arise from the concerted exocytosis of multiple vesicles[18,19].

* To whom correspondence should be addressed.

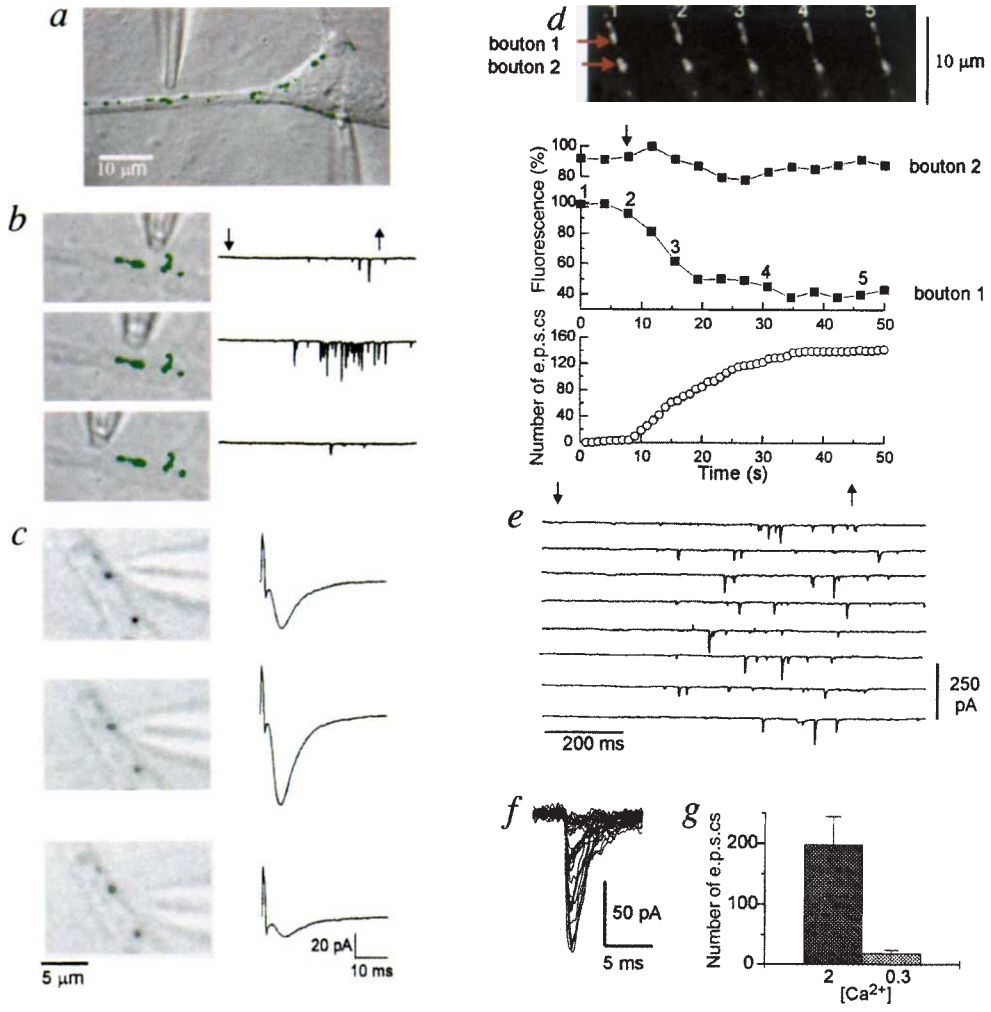

FIG. 1 Stimulation and recording of synaptic activity arising from single boutons, identified, as individual puncta of FM1-43 fluorescence. *a*, Experimental configuration for focal stimulation of boutons of hippocampal neurons in culture. A fluorescence image of FM1-43 dye labelling of presynaptic boutons (green) is shown superimposed on a differential interference contrast image of a postsynaptic hippocampal neuron. A stimulating pipette points downward at the centre of an FM dye spot while a patch electrode is positioned on the cell body for whole-cell voltage-clamp recording (lower right). In most experiments, boutons close to the somatic recording site were chosen for focal stimulation to optimize the space clamp. *b*, Steep dependence of the evoked synaptic current on the position of the pipette tip relative to an area of FM1-43 staining. Vertical arrows indicate onset and termination of an 800 ms puffer application of solution containing 90 mM K^+ in place of Na^+ in normal extracellular medium (2 mM Ca^{2+}). To confine the region of simulation, Ca^{2+} in the bulk extracellular solution was maintained at 0.2 mM. Maximum response (middle trace) obtained when the puffer pipette tip was pointed at the centre of the fluorescent area. Small lateral movements greatly decreased the efficacy of the stimulus (upper and lower traces). *c*, Inward currents at synaptic sites evoked by iontophoretic application of glutamate from a fine-tipped micropipette filled with 250 mM sodium glutamate (pH 7, ~100 MΩ). Iontophoretic current pulses (−100 nA, 1 ms) measured with a virtual ground amplifier. Micropipette was positioned as closely as possible to the FM1-43-stained synapse (middle) or 0.6 μm (top) or 1.6 μm away (bottom). The corresponding current traces include iontophoretic stimulus artefacts (upward-going pulses) and inward currents carried by non-NMDA receptor channels. It was a general finding that response amplitude fell off exponentially, decaying e-fold for lateral pipette movements of ~1 μm, indicating that the glutamate-evoked response arose from stimulation of a single postsynaptic receptor cluster. *d*, Localized effect of high K^+ stimulation. Puffer pipette was directed at the centre of bouton 1. Note that the fluorescence of bouton 1 fell markedly whereas the signal at bouton 2 remained unchanged even after 50 trials of stimulation. Numbers correspond to specific time points in *d*, middle trace. Middle panel, comparison between kinetics of destaining of a single bouton and the accumulation of synaptic events. Repetitive stimulation at 0.5 Hz begins at downward arrow. Percentage fluorescence was determined for boutons 1 and 2 by integrating the fluorescent signal over appropriate pixels (same data as in *c*, with correction for fading, ~1.5% per exposure). The cumulative number of e.p.s.cs (bottom) generally parallels the destaining of bouton 1 (see also ref. 10). *e–g*, Physiological properties of synaptic currents originating from a single bouton. *e*, E.p.s.cs evoked from a single bouton by local application of high K^+ solution (70 mM K^+, 2 mM Ca^{2+}) once every 10 s. Onset and termination of puffer application indicated by vertical arrows. *f*, Variable amplitude but consistently fast time course of single bouton e.p.s.cs. Same neuron as in *e*. *g*, Ca^{2+} dependence of high K^+ response, tested by alternate delivery of 70 mM K^+ solutions containing 2 mM or 0.3 mM Ca^{2+} through a theta glass pipette ($P < 0.01$ by paired *t*–test). Averages are given as mean ± s.e.m. throughout.

METHODS. The procedure for culturing hippocampal neurons was similar to that published previously[8] with the following modification. The cells recovered by centrifugation were plated onto 12-mm round glass coverslips. Culture medium contained: minimal essential medium, glucose 0.5 g l^{-1}, glutamine 0.5 mM, $NaHCO_3$ 2 g l^{-1}, bovine transferrin 100 μg ml^{-1}, insulin 25 μg ml^{-1}, fetal calf serum (FCS) 10%. From the second day in culture, the FCS was reduced to 5% and the medium was supplemented with cytosine-β-arabinofuranoside (4 μM) and B27 medium supplement (2%, GIBCO). The culture medium was replaced twice per week. Whole-cell recordings were obtained from spindle-shaped neurons, presumably CA1 pyramidal neurons, at room temperature (23–25 C). The small experimental chamber (0.25 ml) was continuously perfused (0.25 ml min^{-1}) with Tyrode solution containing (in mM) NaCl 124, KCl 5, $CaCl_2$ 2, $MgCl_2$ 1, glucose 30, HEPES 25 (pH 7.4 with NaOH). Tetrodotoxin 1 μM, D-carboxypiperazin-propyl-phosphonic acid (D-CPP) 5 μM, and picrotoxin 50 μM were added to block action potentials, the NMDA component of synaptic current and Cl^- channels mediating inhibitory synaptic currents. The patch pipette (2.2–3.5 MΩ resistance) contained (in mM): $CsCl_2$ 110, TEA–Cl 10, $MgCl_2$ 5, $CaCl_2$ 1, NaCl 5, EGTA 10, ATP 2, GTP 0.3, HEPES 10 (pH 7.25 with CsOH). The e.p.s.cs were blocked by 6-cyano-7-nitroquinoxaline-2,3-dione (CNQX). The hippocampal neurons were stained with 10 μM FM1-43 in 70 mM [K^+] for 1 min, then washed for >5 min before destaining with local stimulation. The neuron was viewed with a Zeiss IM 35 epifluorescence microscope and illuminated with a 75 W xenon lamp and neutral density transmission filter. The objective was a Nikon ×40 oil immersion lens (0.8–1.3 NA). Fluorescence imaging was done with 425–480 nm excitation and 500–600 nm emission filters, with minimal exposure times (120 ms set-up time plus 33 ms per image) to reduce fading. Images were captured with a Dage 66 SIT camera and stored on a laser disc recorder. An IBM-PC 486 computer was used to control the shutter and puffer application of test solutions, and for acquisition of video frames and whole-cell current records and their off-line analysis. For studies of the time course of destaining, the boundaries of the dye-stained region were delineated for the first image, and fluorescent intensity was averaged over the pixels within the same boundary for all images. The intensity data were corrected for illumination-induced fading, using a linear time course derived from fluorescent spots well away from the site of local stimulation.

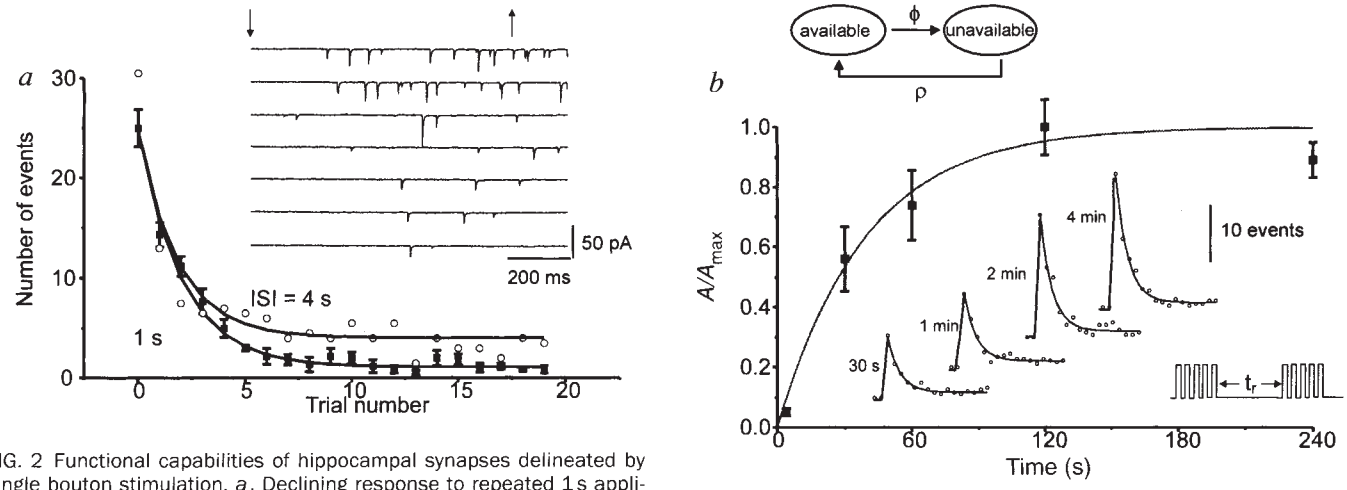

FIG. 2 Functional capabilities of hippocampal synapses delineated by single bouton stimulation. *a*, Declining response to repeated 1 s application of high K^+/Ca^{2+} solution, delivered at 0.2 Hz (interstimulus interval, ISI = 4 s) and 0.5 Hz (ISI = 1 s). Inset shows representative records for 0.5 Hz stimulation. *b*, Kinetics of recovery of responsiveness following a varying rest interval, t_r. The time course of recovery was determined by plotting the ratio of the response area after a variable rest period (A) to that after a 4 min rest period (A_{max}). Data from multiple runs from each of three individual boutons were averaged. Smooth curve is a single exponential fit ($\tau_r = 39.1$ s). Also shown are averaged responses following recovery intervals of 0.5, 1, 2 and 4 min ($n = 3$ trials at each interval). Inset, a simple model which generates the theoretical curves in *a* and *b*. Vesicles recycle between unavailable and available pools; the available pool includes both readily releasable and reserve vesicles. The forward transition (probability per trial, ϕ) incorporates vesicle docking and other steps up to and including transmitter release, whereas the reverse transition (probability per trial, ρ) represents endocytosis and repriming. The variable N designates the number of events that can be generated by the available vesicular pool in the absence of endocytotic retrieval and N_a is the initial (maximal) value of N after a long period of rest. The curves were generated by an iterative program which allows for the pulsatile nature of the stimuli; they are essentially exponentials, of the form $v = (v_0 - v_\infty)e^{t/\tau_d} + v_\infty$, where v the number of events per trial, $v_0 = N_a\phi$, $v_\infty = N_a\phi\rho/(\phi+\rho)$, $\tau_d = (\phi+\rho)^{-1}$. The parameters for the curves are $N_a = 66$, $\phi = 0.375$ per trial, ρ(ISI = 1 s) = 0.017 per trial, ρ(ISI = 4 s) = 4, ρ(ISI = 1 s) = 0.068 per trial (this value is plotted as the lowermost data point in *b*). In compiled results, N_a was not correlated with the proximity of the stimulated bouton to its nearest neighbour, as expected for e.p.s.cs generated by a single bouton. An alternative to this depletion model is a scheme, discussed in ref. 16, where the response to repetitive stimuli declines because of build-up of an inhibitory factor and recovery reflects its disappearance.

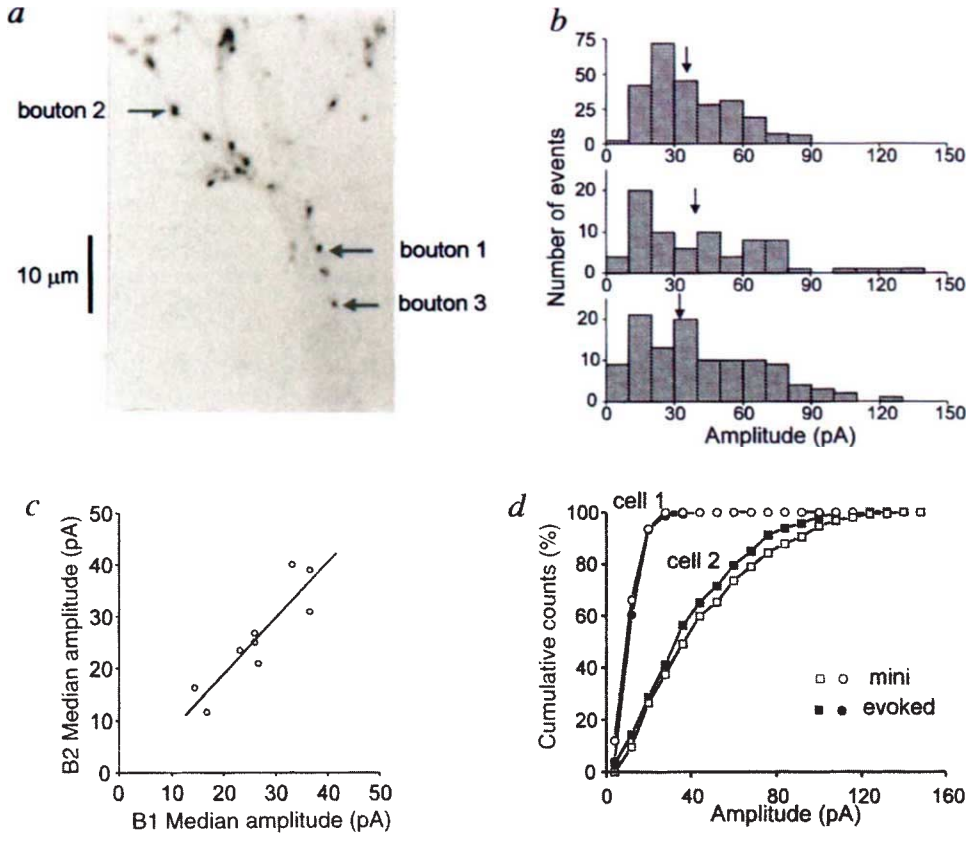

FIG. 3 Comparison of single bouton responses stimulated at multiple locations on the same postsynaptic neuron. *a*, Positions of three sites of single bouton stimulation on the dendritic tree. *b*, Corresponding amplitude histograms of e.p.s.cs evoked at the three sites. Note similarity in median amplitudes (vertical arrows), 36.5, 39.1 and 31.2 pA for boutons 1, 2 and 3, respectively. $V_m = -70$ mV. *c*, Correlation between median e.p.s.c. amplitudes from multiple boutons within same cell (slope = 1.08, $r = 0.90$, $P < 0.001$). Data from pairs of boutons in 7 cells, and three boutons in 2 cells as in *a* and *b*. Note large variation in median e.p.s.c. size among different cells. *d*, Comparison of amplitude histograms (cumulative) of evoked e.p.s.cs and spontaneous miniature e.p.s.cs. Although the distributions of evoked and mini amplitude are not significantly different for either of the two cells illustrated ($P > 0.1$ by Kolmogorov–Smirnov test), there is a striking difference between cells. In collected results from 10 cells, median amplitudes of minis were highly correlated with those of evoked e.p.s.cs (slope = 0.70, $r = 0.81$, $P < 0.005$). The spontaneous events were, on average, slightly smaller than the evoked events, and also slightly slower in both 20–80% rise time (0.59 ± 0.02 versus 0.51 ± 0.03 ms) and decay time constant (3.67 ± 0.20 versus 3.19 ± 0.19 ms) ($n = 10$ cells). These differences would be expected for spontaneous synaptic events originating from various positions within the dendritic tree, including sites where the voltage clamp is not as effective as at the site of focal stimulation.

The ability to stimulate individual boutons allowed us to compare the behaviour of multiple synapses onto the same postsynaptic neuron. Figure 3 shows dye-stained boutons at three different locations on a dendrite tree (*a*) and their individual e.p.s.c. amplitude distributions (*b*). Although broad, the distributions appear similar in median amplitude (arrows). This similarity was found consistently in pairs of single bouton recordings (Fig. 3*c*): the median amplitude values for individual neurons were nearly the same even though these values varied widely from one cell to another (14–40 pA). The comparison of evoked responses has the advantage that these can be pinpointed to specific postsynaptic locations. We also compared events elicited at one synaptic site with spontaneous miniature e.p.s.cs (minis), presumably reflecting transmitter release at sites throughout the dendritic tree. The cumulative distribution of spontaneous mini size was very similar to that of K^+/Ca^{2+}-evoked e.p.s.cs (Fig. 3*d*), in cells giving small averaged synaptic responses (cell 1) or large ones (cell 2). This was a general finding (Fig. 3 legend). Evidently, the broad dispersion of mini amplitudes does not reflect great variation from one synapse to the next but can be largely explained by intrinsic variability at individual synapses.

The wide range of average unitary event size across different cells prompted us to look for a possible correlation with the degree of synaptic innervation. Figure 4*a* shows representative examples of neurons with relatively low or high densities of presynaptic boutons (same cover slip). The e.p.s.cs were substantially larger in the neuron with low synapse density than in the densely innervated neuron (Fig. 4*b*). This relationship was confirmed in compiled results ($n = 19$ cells, Fig. 4*c*). Median e.p.s.c. amplitude varied inversely with active synapse density as gauged by the percentage of pixels within the dendritic regions brightly stained with FM1-43. In contrast, there was no significant correlation between e.p.s.c. size and culture age ($P > 0.4$, Fig. 4*d*). Although the median e.p.s.c. size was clearly larger in the more sparsely innervated cells, it was consistently small (<15 pA) when >10% of the dendrite surface area was covered with fluorescent spots (Fig. 4*c*).

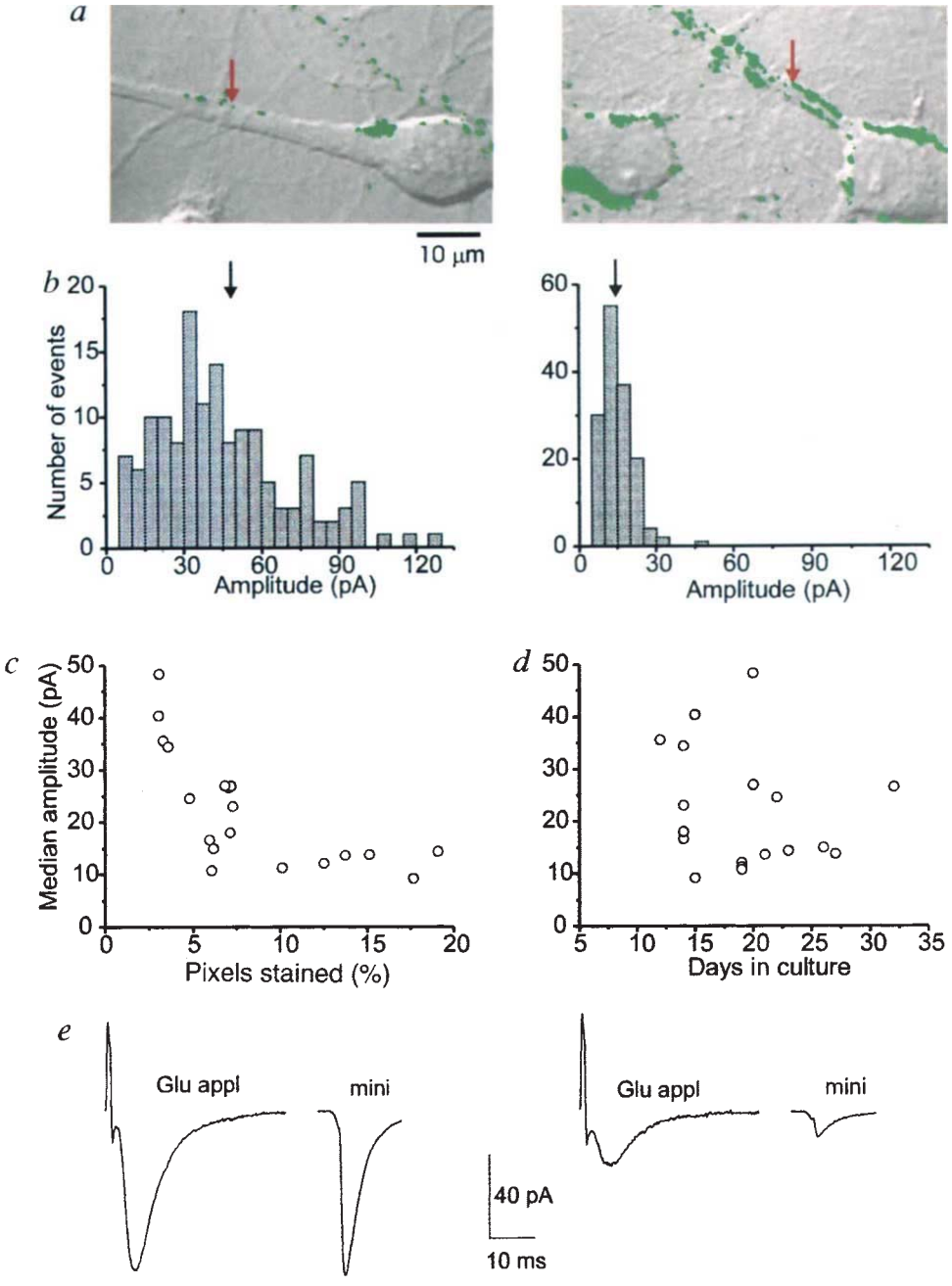

FIG. 4 Single bouton responses are inversely correlated in size with the density of active synapses. *a*, Examples of cultured hippocampal neurons with low and high densities of active boutons as detected with FM1-43 staining (same coverslip). Arrows indicate the location of stimulation sites. *b*, Amplitude histograms of evoked e.p.s.cs from the neurons shown in *a*. Arrows indicate the median e.p.s.c. sizes (45 and 14 pA, respectively). *c*, Median amplitude of e.p.s.cs plotted against the density of active synapses (19 cells). Density was estimated for each cell by examinining a DIC image of the recorded neuron and considering a standard length of proximal dendrite extending up to 50 μm away from the soma. The number of pixels displaying fluorescent intensity larger than predefined threshold were expressed as a percentage of the total number of pixels in the defined dendritic area (abscissa). *d*, Median amplitude of e.p.s.cs plotted against the age of the neuronal culture. No significant correlation was found ($P = 0.44$ by linear regression). *e*, Comparison of responses to focal glutamate application at a single postsynaptic locus and averaged spontaneous minis, in neurons with low synapse density (left) and high synapse density (right). Averaged traces, same iontophoretic electrode, same cover slip; see Fig. 1 for experimental details. Note that the size of the glutamate-evoked current varies greatly, in parallel with the average mini amplitude, in inverse correlation with synaptic density.

This striking pattern of behaviour could conceivably arise from either presynaptic mechanisms (variations in vesicular glutamate or the number of vesicles contributing to an e.p.s.c.), or postsynaptic ones (variations in receptor density or type). As a test for a possible presynaptic mechanism, we examined the kinetics of vesicular depletion during trains of high K^+ stimuli. No significant difference was found in N_a, ϕ or ρ in neurons with high or low innervation density (Fig. 4 legend). Thus there was no hint of a more concerted release of vesicles from a finite pool as an explanation for the larger e.p.s.cs. To test for possible differences in postsynaptic responsiveness, we compared the responses to standardized iontophoretic application of glutamate[9] with NMDA receptors blocked in sparsely and densely innervated cells. Figure 4*e* illustrates focal glutamate responses in neurons with low (3.1%, left) and high (16.2%, right) densities (same cover slip). The amplitudes of the glutamate responses were strikingly different, as with disparately sized average spontaneous minis from the same cells. In collected results, glutamate response amplitude and mini e.p.s.c. size each varied widely, but were highly correlated ($n=8$ cells, $r=0.94$, $P<0.001$). These experiments demonstrate the importance of postsynaptic factors in the variation in unitary e.p.s.c. size. The inverse relationship of postsynaptic responsiveness with synapse density may be advantageous in allowing neurons to compensate for augmented innervation, adjusting synaptic input to the dynamic range of the spike-firing decision and preventing overexcitability and toxicity. Simple competition among postsynaptic sites for a fixed number of glutamate receptors cannot be the whole explanation, because e.p.s.c. size is maintained at an apparent lower limit whereas innervation density increases twofold (Fig. 4*c*). The lower limit might correspond to quantal spacing in hippocampal slices[14,20–22].

In establishing an approach for focal stimulation of transmitter release from individual presynaptic boutons, our experiments provide new information about the functional capabilities of single synapses in responding to various patterns of stimulation. Single boutons are able to generate in the range of 40–160 e.p.s.cs in the absence of a slow recovery process that we attribute to vesicular recycling[6,7]. Although the distribution of unitary e.p.s.c. size is broad[1], the average size is very similar at different synaptic loci on an individual neuron. This bouton-to-bouton consistency offers functional advantages for processing of information from multiple input pathways, and augurs well for quantal analysis of evoked transmission[14,20–22]. Future exploration of how a CNS neuron manages to control the amplitude and uniformity of the glutamate response across a multitude of postsynaptic sites will no doubt be helped by the ability to study neurotransmission at individual synapses. □

Received 16 November 1994; accepted 15 March 1995.

1. Bekkers, J. M., Richerson, G. B. & Stevens, C. V. *Proc. natn. Acad. Sci. U.S.A.* **87,** 5359–5362 (1990).
2. Lavidis, N. A. & Bennett, M. R. *J. Physiol., Lond.* **454,** 9–26 (1992).
3. Lisman, J. E. & Harris, K. M. *Trends Neurosci.* **16,** 141-147 (1993).
4. Edwards, F. *Nature* **350,** 271–272 (1991).
5. Raastad, M., Storm, J. F. & Andersen, P. *Eur. J. Neurosci.* **4,** 113–117 (1992).
6. Betz, W. J., Mao, F. & Bewick, G. S. *J. Neurosci.* **12,** 363–375 (1992).
7. Ryan, T. A. *Neuron* **11,** 713–724 (1993).
8. Malgaroli, A. & Tsien, R. W. *Nature* **357,** 134–139 (1992).
9. Jones, K. A. & Baughman, R. *Neuron* **7,** 593–603 (1991).
10. Betz, W. J. & Bewick, G. S. *J. Physiol., Lond.* **460,** 287–309 (1993).
11. Katz, B. & Miledi, R. *J. Physiol., Lond.* **189,** 535–544 (1967).
12. Dodge, F. A. Jr & Rahamimoff, R. *J. Physiol., Lond.* **193,** 419–432 (1967).
13. Wu, L. G. & Saggau, P. *Neuron* **12,** 1139–1148 (1994).
14. Jonas, P., Major, G. & Sakmann, B. *J. Physiol., Lond.* **472,** 615–663 (1993).
15. Silver, R. A., Traynelis, S. F. & Cull-Candy, S. G. *Nature* **355,** 163–166 (1992).
16. Stevens, C. F. & Tsujimoto, T. *Proc. natn. Acad. Sci. U.S.A.* **92,** 846–849 (1995).
17. Horrigan, F. T. & Bookman, R. J. *Neuron* **13,** 1119–1129 (1994).
18. Tong, G. & Jahr, C. E. *Neuron* **12,** 51–59 (1994).
19. Stevens, C. F. *Cell* **72** (suppl.), 55–63 (1993).
20. Edwards, F. A., Konnerth, A. & Sakmann, B. *J. Physiol., Lond.* **430,** 213–249 (1990).
21. Larkman, A., Stratford, K. & Jack, J. *Nature* **350,** 344–347 (1991).
22. Liao, D., Jones, A. & Malinow, R. *Neuron* **9,** 1089–1097 (1992).

ACKNOWLEDGEMENTS. We thank I. Bezprozvanny, K. Deisseroth, B. Hille, D. Johnston, A. D. Randall, F. E. Schweizer, C. F. Stevens and R. S. Zucker for their comments on earlier versions of this paper, S. J. Smith for valuable help with early software development, and F. Mao for a gift of FMI-43 and helpful discussions. This work was supported by the Mathers Charitable Trust, NINCDS and the Silvio Conte-NIMH Center for Neuroscience Research at Stanford.

Altered immune responses in mice lacking inducible nitric oxide synthase

Xiao-qing Wei*†, Ian G. Charles†, Austin Smith‡, Jan Ure‡, Gui-jie Feng*, Fang-ping Huang*, Damo Xu*, Werner Muller§, Salvador Moncada† & Foo Y. Liew*‖

* Department of Immunology, University of Glasgow, Glasgow G11 6NT, UK
† The Wellcome Research Laboratories, Beckenham, Kent BR3 3BS, UK
‡ Gene Targeting Laboratory, Centre for Genome Research, University of Edinburgh, King's Buildings, Edinburgh EH9 3JQ, UK
§ Institute for Genetics, University of Cologne, Weyertal 121, D-50931 Cologne, Germany

NITRIC oxide (NO) is important in many biological functions[1–5]. It is generated from L-arginine by the enzyme NO synthase (NOS). The cytokine-inducible NOS (iNOS) is activated by several immunological stimuli, leading to the production of large quantities of NO which can be cytotoxic[6]. To define the biological role of iNOS further, we generated iNOS mutant mice. These are viable, fertile and without evident histopathological abnormalities. However, in contrast to wild-type and heterozygous mice, which are highly resistant to the protozoa parasite *Leishmania major* infection, mutant mice are uniformly susceptible. The infected mutant mice developed a significantly stronger Th1 type of immune response than the wild-type or heterozygous mice. The mutant mice showed reduced nonspecific inflammatory response to carrageenin, and were resistant to lipopolysaccharide-induced mortality.

The iNOS gene was disrupted in embryonic stem cells which were then used to produce germline chimaeras. F_1 mice (129 × MF1) heterozygous for the mutation were bred to obtain homozygotes for the disrupted iNOS gene. Loss of the wild-type allele was confirmed by Southern blotting (Fig. 1*a*). Homozygous animals were viable and fertile, and there was no evidence of histopathology within the major organs examined (data not shown). Interbreeding of (129 × MF1) homozygous mutant mice gave rise to a stock of mice that were used for the following experiments. Homozygous mice were compared with sex- and age-matched animals of wild-type MF1 mice or heterozygous breeding.

Peritoneal macrophages are the best-characterized source of iNOS in the mouse. Macrophages from wild-type or heterozygous mice, when stimulated with interferon(IFN)-γ and lipopolysaccharide (LPS) *in vitro*, expressed iNOS messenger RNA and iNOS protein, and produced substantial amounts of NO, measured as nitrite in the culture supernatant. In contrast, similarly stimulated macrophages from the mutant mice did not contain the normal 4.0-kilobase (kb) iNOS mRNA, but did contain an altered hybridizing species of 4.5 kb (Fig. 1*b*). The stimulated cells showed no detectable iNOS protein by western blot (Fig. 1*c*), and produced only a background concentration of nitrite, not significantly different from that produced by unstimulated cells in 24 to 48 h cultures (Fig. 1*d*).

The wild-type mice and the heterozygous mice were highly resistant to *L. major* infection, and all animals achieved spontaneous healing after footpad infection with 10^6 promastigotes. In contrast, the mutant mice were highly susceptible to the infection (Fig. 2) and developed visceral disease by postinfection day 70 (data not shown). There was no significant difference in lesion size between the three groups of mice until 5 weeks after infection, indicating that the innate response, possibly under the

‖ To whom correspondence should be addressed.